

1  
2  
3  
4  
5  
6  
7  
8  
9  
10  
11  
12  
13  
14  
15  
16  
17  
18  
19  
20  
21  
22  
23  
24  
25  
26  
27  
28  
29  
30  
31  
32  
33  
34  
35  
36  
37  
38  
39  
40  
41  
42  
43  
44  
45  
46  
47

## Tissue Resolved, Gene Structure Refined Equine Transcriptome

Mansour, T.A.\*<sup>1,2</sup>, Scott, E.Y.\*<sup>3</sup>, Finno, C.J.<sup>1</sup>, Bellone, R.R.<sup>4</sup>, Mienaltowski, M.J.<sup>3</sup>, Penedo, M.C.<sup>4</sup>, Ross, P.J.<sup>3</sup>, Valberg, S.J.<sup>5</sup>, Murray, J.D.<sup>1,3</sup>, Brown, C.T.<sup>1</sup>.

<sup>1</sup> Department of Population Health and Reproduction, University of California, Davis, <sup>2</sup> Department of Clinical Pathology, College of Medicine, Mansoura University, Egypt <sup>3</sup> Department of Animal Science, University of California, Davis, <sup>4</sup> Veterinary Genetics Laboratory, University of California, Davis, <sup>5</sup> Large Animal Clinical Sciences, Michigan State University, College of Veterinary Medicine

\*Both authors contributed equally to this manuscript

**To be submitted to BMC Genomics**

## 48 **Abstract**

49 *Background:* Transcriptome interpretation relies on a good-quality reference transcriptome for accurate  
50 quantification of gene expression as well as functional analysis of genetic variants. The current  
51 annotation of the horse genome lacks the specificity and sensitivity necessary to assess gene expression  
52 especially at the isoform level, and suffers from insufficient annotation of untranslated regions (UTR).  
53 We built an annotation pipeline for horse and used it to integrate 1.9 billion reads from multiple RNA-  
54 seq data sets into a new refined transcriptome.

55 *Results:* This equine transcriptome integrates eight different tissues from 59 individuals and improves  
56 gene structure and isoform resolution while providing considerable tissue-specific information. We  
57 utilized four levels of transcript filtration in our pipeline, aimed at producing several transcriptome  
58 versions that are suitable for different downstream analyses. Our most refined transcriptome includes  
59 36,876 genes and 76,125 isoforms, with 6474 candidate transcriptional loci novel to the equine  
60 transcriptome.

61 *Conclusions:* We have employed a variety of descriptive statistics and figures that demonstrate the  
62 quality and content of the transcriptome. The equine transcriptomes that are provided by this pipeline  
63 show the best tissue-specific resolution of any equine transcriptome to date and can serve several types  
64 of downstream analyses.

65

66 **Keywords:** Equine transcriptome, tissue-specificity, RNA-seq

67

## 68 **Introduction**

69 Transcriptomics is rapidly evolving from a focus on novel gene identification to resolving structural  
70 gene details. The transcriptomes of better-studied organisms, such as *Drosophila*, mouse and human  
71 have been updated to accommodate for this transition [1-3]. However, for less well characterized

72 animals, such as the horse, there is often only annotation of a single variant of a gene with insufficient  
73 annotation of multiple splice variants, UTR extensions and non-protein coding RNA. This lack of  
74 information can challenge subsequent differential gene expression analyses and functional studies. There  
75 have been several attempts to improve the equine transcriptome with single tissue transcriptomes from  
76 lamellar tissue [4] or peripheral blood mononuclear cells [5] and from pooled composites of various  
77 tissues [6, 7], however a broader effort defining and integrating many tissue-specific transcriptomes and  
78 obtaining the library depth and strand information required to capture gene complexity is still needed.

79 ENSEMBL and NCBI provide publically available annotations for several vertebrate genomes  
80 including horses [8]. Both underlying annotation pipelines integrate homology search and *ab initio*  
81 prediction however accurate UTR prediction and isoform recognition require species-specific  
82 transcriptional evidence [9, 10]. For this equine transcriptome, the transcriptional evidence provided by  
83 total RNA sequencing (RNA-seq) was the basis of our gene annotation. This approach permits more  
84 reliable discovery of novel genes and isoforms, extension of UTRs and the flexibility necessary to  
85 establish a balance between sensitivity and specificity of gene detection for downstream applications.

86 Our annotation integrates the benefits of increased depth in reads and strand-specificity, for some  
87 tissues, as well as using a range of tissues from many horses, which allows tissue-specific  
88 transcriptomes to be extracted. We have incorporated RNA-seq from a diverse set of 8 tissues ranging  
89 from the central nervous system (CNS), skin and skeletal muscle tissues in adults to the inner cell mass  
90 (ICM) and trophectoderm (TE) in embryonic tissues (Table 1). The diversity in age, sex and tissue of the  
91 samples included in our assembly supply the equine transcriptome with its best spatiotemporal  
92 resolution and most complete gene UTR definition to date.

93 We recognize that availability of annotation criteria and integration of transcriptome data is  
94 paramount for systematically improving the equine transcriptome. Our goal is to encourage equine

95 researchers to incorporate their transcriptomic data using our pipeline as the common annotation  
96 pipeline and our initial transcriptomes as a reference framework. We intend to continue improving  
97 equine gene annotation through better UTR definition, isoform splicing characterization and novel gene  
98 identification. The annotation presented in this paper will improve the gene structure definition in  
99 current databases and the accuracy of downstream analyses, including both differential gene expression  
100 analysis and genetic variant annotation in the horse.

101

102

## 103 **Results**

104

### 105 *Overall Mapping Statistics and Gene Counts After Filtration*

106

107 RNA-seq of 59 samples in 12 libraries from 8 different horse tissues provided 1.9 billion  
108 fragments and 364 Gb of sequence bases. A summary of the library preparation, number of horses per  
109 library and total number of fragments and bases provided by each tissue library can be found in Table 1.  
110 The overall average mapping rate for Tophat2 was ~83% with concordance rates ranging from 29% to  
111 89% (average 75%) for paired end libraries. Concordance rates seem to be affected by the type of  
112 library preparation, where polyA selected and strand-specific libraries have the best rates. Library  
113 specific mapping rates can be found in Supplementary Table 1. The initial Cufflinks assembly identified  
114 117,019 genes/211,562 transcripts. After this initial analysis we applied four steps of filtration (Figure  
115 1). Primary filtration of transcripts removed the likely pre-mRNA fragments by eliminating single exon  
116 transcripts that were present within introns or overlapping with exons of other multi-exon transcripts.  
117 After primary filtration there were 75,102 genes/162,261 transcripts. The second filter was implemented

118 to remove isoforms likely to be experimental artifacts by excluding low abundant transcripts with less  
119 than 5% of total expression for their locus. The remaining 114,830 transcripts represented 75,375 genes.  
120 In the third filter, non-coding transcripts that lack any supporting evidence from NCBI or ENSEMBL  
121 annotations, non-horse gene models (“Other RefSeq” and “TransMap RefGene” UCSC tracks) or *ab*  
122 *initio* predictions (“Augustus”, “Geneid”, “Genscan” and “N-SCAN” UCSC gene prediction tracks)  
123 were excluded. This third filtered version of the transcriptome has 76,323 transcripts in 37,062 genes.  
124 The last filter was for removing likely erroneous transcripts. The mtDNA in mammals is known for gene  
125 overlapping and polycistronic expression [11], permitting inaccurate prediction of mitochondrial  
126 transcripts by Cufflinks; we therefore excluded the mitochondrial contigs from our filtered assembly.  
127 Also, short transcripts less than 201bp (192 transcripts in 184 genes) were removed because they are  
128 more likely to represent repetitive sequences or incomplete gene fragments. Once erroneous transcripts  
129 were removed, our final refined version of the transcriptome contained 36,876 genes (76,125 transcripts)  
130 including 15,343 single exon transcripts, 8,808 two-exon transcripts, and 51,974 transcripts with three or  
131 more exons. A version of our refined transcriptome that is merged with the NCBI and ENSEMBL  
132 annotations, with redundant transcripts removed, is also available. This is the most comprehensive  
133 product of our pipeline and is valuable for differential gene expression analysis in tissues other than  
134 those provided in our assembly. Summary statistics including N50, number of genes and Mb and  
135 average length of fragment for all six versions of the transcriptome can be found in Supplementary  
136 Table 2.

### 137 *Comparison between Our Transcriptome and Currently Available Equine Transcriptomes*

138

139 We performed a comparison between our transcriptome and gene models from NCBI,  
140 ENSEMBL and two published equine transcriptomes, that we refer to as Hestand [7] and ISME [5]

141 (Table 2 and Supplementary Table 3). In our comparisons, transcripts sharing one or more splice  
142 junctions are considered similar but only those with identical intron chains are matching. The  
143 comparison shows that the matching transcripts between our refined transcriptome and NCBI annotation  
144 are greater than 2.5-fold in number those matching the ENSEMBL annotation. However the highest  
145 number of matching transcripts occurred with the ISME transcriptome with 12,849 transcripts (Figure  
146 2A). About 50% of the refined transcripts have a similar match in all the public transcriptomes.  
147 Evidence of improvements to the annotation of genes with a similar match to other assemblies can be  
148 found in genes such as *MUTYH*, where the three major isoforms annotated in humans [12] are now  
149 distinguishable in the horse (Figure 2B). The gene *CYP7A1* is another example where a novel first exon  
150 has been annotated and extended in our version of the transcriptome [13] (Figure 2C). About 20% and  
151 28% of the refined transcripts are novel when compared to NCBI and ENSEMBL annotations  
152 respectively. Combined, there are 22,641 transcripts in candidate novel loci. Our approach of applying  
153 four successive steps of filtration strictly qualifies our novel isoforms as transcripts with ORFs or exonic  
154 overlap with candidate gene models. Mainly, novel transcripts contained within introns of other genes  
155 were excluded to avoid artifacts from retained intronic reads, common in rRNA depleted libraries. Using  
156 NCBI as a reference for comparison, our novel transcripts from the refined transcriptome have no bias  
157 towards any particular chromosome after accounting for chromosome size (Supplementary Figure 1). In  
158 order to calculate the gene and isoform detectability of our transcriptome compared to current  
159 annotation, we calculated sensitivity and specificity [14] between our transcriptome and a reference and  
160 found that, using NCBI as the reference, our transcriptome had a 78.8% sensitivity and 23.8%  
161 specificity at the base level and a 32% sensitivity and 21.1% specificity at the locus level. Detailed  
162 pairwise assessment for all equine annotations can be found in Supplementary Table 4. We developed a  
163 statistic to assess the conflict between different assemblies, termed “complex loci”, which refer to the

164 loci that represent one gene locus in one transcriptome and two or more gene loci in another. Our  
165 transcriptome has 1355 and 997 transcripts that were considered complex loci between our  
166 transcriptome and NCBI and ENSEMBL, respectively. The Hestand transcriptome, however, has fewer  
167 with 660 and 798 complex loci when compared to NCBI and ENSEMBL, respectively. The ISME  
168 transcriptome has substantially more, with 1546 and 1226 complex loci when compared to NCBI and  
169 ENSEMBL, respectively.

170

### 171 *UTR extension*

172

173 To test the effect of the new assembly on the UTRs of known genes, we identified the protein  
174 coding isoforms sharing the exact intron chain with NCBI isoforms, which yielded 9736 isoforms from  
175 7419 genes. The difference in the total length of each transcript was then calculated and we found that  
176 we extended the length of 8899 isoforms (6817 genes) by 29.7 Mb in total. 831 isoforms (718 genes)  
177 lost 0.3 Mb in total with an average of 0.4 kb per isoform, while 6 isoforms did not change.

178

### 179 *Gene and Isoform Distinctions between Tissue-Specific Transcriptomes*

180

181 We selected genes with high expression (a sum of TPMs across all tissues above 200) and  
182 substantial expression differences across tissues (a standard deviation above 200). Unsupervised  
183 hierarchical clustering grouped genes that may be co-expressed as well as illustrating the relationship  
184 between the tissue-specific transcriptomes. As expected, the transcriptomes from the three central  
185 nervous system (CNS) tissues clustered together, as did the two embryonic tissues, with the skin and  
186 skeletal muscle furthest from these clusters (Figure 3A). Blocks of genes showing uniquely high

187 expression in a given tissue were further annotated with NCBI gene names and then summarized with  
188 Panther biological processes annotations. The top two Panther pathways (lowest p-values) for each of  
189 these gene blocks are reported in the text below, with the corresponding p-values (p) and fold-  
190 enrichment vales (FE). The full Panther annotation tables are detailed in Supplementary Table 5. The  
191 CNS cluster contained overrepresented processes regarding brain function and development: nervous  
192 system development (p=2.10E-06, FE=7.12) and neurogenesis (p=9.36E-05, FE=7.73). The retina  
193 contained processes consisting of photoreception and visual perception: phototransduction (p=3.52E-08,  
194 FE=80.75) and visual perception (p=3.69E-18, FE=37.64). The skeletal muscle encompassed genes  
195 pertaining to muscle physiology and assembly: muscle contraction (p=1.48E-27, FE =57.58) and  
196 myofibril assembly (p=6.05E-11, FE=72.8). The embryonic tissues have the most general processes  
197 assigned to their distinct clusters: translation (p=1.15E-11, FE=16.35) and peptide biosynthetic  
198 processes (p=1.95E-11, FE=15.8). And finally, the skin consisted of processes concerning epithelial  
199 organization and production: intermediate filament organization (p=1.69E-07, FE > 100) and skin  
200 development (p=1.89E-09, FE=22.49).

201 When attention is given to the isoforms showing unique presence or sole absence in a tissue, the  
202 retina and cerebellum possess the most isoforms that are uniquely present, with the retina also  
203 containing the largest amount of solely absent isoforms (Figure 3B). The uniquely present transcripts in  
204 the retina have Panther annotations of visual perception (p=2.96E-23, FE=7.47) and photoreceptor cell  
205 differentiation (p=1.59E-09, FE=7.56) and in the cerebellum nervous system development (p=3.08E-09,  
206 FE=1.85) and generation of neurons (p=1.72E-08, FE=2.02). Full Panther annotation tables of  
207 transcripts uniquely present in tissues can be found in Supplementary Table 6. The transcripts solely  
208 absent from the retina pertain mainly to positive regulation of DNA replication (p=2.49E-03, FE=3.53)  
209 and anatomical structure development (p=2.72E-19, FE=1.48). Full Panther annotation tables of



210 transcripts solely absent in tissues can be found in Supplementary Table 7. Utility of these isoforms, in  
211 terms of expression, is strongest in the skin, retina, skeletal muscle and to a small extent the cerebellum  
212 (Figure 3B). Despite these differences in unique isoforms, multi-exons transcripts and multi-transcript  
213 loci, the splicing rate across tissues, as calculated by Cuffcompare [15], ranges from 1.7 to 1.9 (Table 3).

214 Nuclear coding versus mitochondrial encoded genes were parsed out per tissue to determine how  
215 much of the sequencing resources are allocated to genes of the mitochondria (Figure 3C), with the  
216 conclusion that the brainstem, spinal cord, embryonic tissues and skeletal muscle exhibit the largest  
217 proportions of transcriptional output devoted to mitochondrial genes.

218

### 219 *Classification and Annotation of Novel Genes*

220

221 In total there were 22,640 novel transcripts, with varying levels of support from current equine  
222 annotations (Figure 4A). Classification of these candidate novel genes was necessary to better describe  
223 our novel gene identification and aid in interpreting the degree of support available to each category.  
224 Three categories of novel genes based upon the supportive evidence within and across species were  
225 made with each successive category being less supported by equine or orthologous gene models. Our  
226 first category of novel genes contains those missing from NCBI and/or ENSEMBL annotations, but  
227 supported by either NCBI, ENSEMBLE, Hestand or ISME annotations (Category I). The second group  
228 of novel genes were novel to all public equine annotations, but conserved by means of orthologous gene  
229 similarity or supported by possible gene prediction (Category II). The third category of novel genes  
230 were unsupported by any candidate gene models, but had an ORF (Category III). Category I has a total  
231 of 8459 transcripts, with 2/3 of these transcripts novel to the ENSEMBL annotation (Supplementary  
232 Figure 2). Another 1849 transcripts in this category are absent in both NCBI and ENSEMBL

233 annotations, yet supported by Hestand or ISME annotations. Homology with the SWISS-prot database  
234 identified at least one significant ( $p < 1E-10$ ) hit for almost half the transcripts in this Category I  
235 (Supplementary Table 8). The second category has 7494 transcripts that – unless on the opposite strand  
236 - do not overlap with known gene models in public annotations. Annotation of these transcripts was  
237 performed partially by testing overlap with non-horse gene models and also by homology search. Only  
238 16% of these transcripts have significant hits against the SWISS-prot database (Supplementary Table 8).  
239 The third category of novel genes includes 6687 transcripts with an ORF as the only functional support  
240 for these transcripts. The first category of novel genes shows the most diverse distribution of exon  
241 numbers comprising the genes (ranging from 1 to 28), whereas the unsupported genes contained mainly  
242 single exon genes (Figure 4B). The expression analysis of the three novel gene categories shows a clear  
243 reduction of cumulative expression from category I to III. There was also an obvious tissue-specific  
244 pattern in the expression of novel genes. Supported novel genes (Category I) had the highest expression  
245 in the cerebellum. However, when looking at only the second category of novel genes, the embryo  
246 contributed the highest expression of novel transcripts. Category III novel transcripts mainly consisted  
247 of single exon transcripts and showed similarly low expression across all tissues (Figure 4C).

248

## 249 **Discussion**

250 Using RNA-seq from fifty-nine horses across eight tissues has allowed us to capture  
251 transcriptome complexity and provide spatial resolution in terms of tissue-specificity in manner that  
252 exceeds any current equine annotations. Our descriptive statistics and accessible pipeline make this  
253 project open to modifications and further integration of transcriptomes.

254 RNA-seq based transcriptomes are prone to false inflation of gene numbers for several reasons.  
255 Technical limitations such as limited sequencing read length and amplification errors, false splicing

256 events, and assembler deficiencies are among several reasons of misassembly. Pervasive transcription is  
257 another predominant source of such inflation [16-18]. Some types of sequencing libraries increase the  
258 problem as well; for example rRNA depletion inflates the assembly with primary transcripts and false  
259 isoforms exhibiting intronic retention [19]. Our pipeline takes these factors into account and runs  
260 unguided by previous transcriptome annotations with several transcript filtration steps that reduce  
261 inclusion of inaccurate transcripts, while retaining the sensitivity for novel transcript detection. The  
262 effect of this procedure can be seen by comparing the gene numbers between our initial unfiltered and  
263 final filtered transcriptomes, where gene inflation was reduced by 68% (Table 2) and our final refined  
264 transcriptome contained 36,876 genes and 76,125 isoforms.

265         Although not indicative of transcriptome quality, we calculated specificity, as a measure of  
266 difference between our transcriptome and other annotations, and sensitivity, which indicates how our  
267 transcriptome covers another annotation. These parameters demonstrate that our aggressive filtering  
268 does sacrifice sensitivity at the locus level only by a margin of approximately 5%, and increases our  
269 specificity often by more than 10%, relative to NCBI and ENSEMBL (Supplementary Table 4). We  
270 have a comparable sensitivity to the Hestand transcriptome, which could be explained by adopting strict  
271 filtering approaches in both pipelines. However, the numbers of unstranded and multi-exon transcripts in  
272 the Hestand transcriptome relative to our refined version serve as the more discriminating statistics. We  
273 have approximately six fold less unstranded transcripts and more than double the multi-exon transcripts  
274 (Table 2). Regarding how our transcriptome compares to the other recent equine ISME assembly [5],  
275 which is ENSEMBL annotation guided, we have three times more matching transcripts to the ISME  
276 assembly than to the ENSEMBL annotation itself (Figure 2A), suggesting significant improvement  
277 made by the ISME annotation. However their improvements are impaired by false inflation in the  
278 number of genes identified due to presenting most of the transcripts in two copies representing the

279 forward and reverse strands. This inflation of the ISME annotation can explain why it has different  
280 statistics from Hestand as well as our new transcriptome. Hestand et al (2015) also observed a bias  
281 towards single exon genes, which represented approximately 55% of their whole transcriptome [7]. Our  
282 native assembly identified similar percentage of single exon transcripts, however those numbers went  
283 down to 20% after filtration of single exon pre-mRNA. Our statistic, complex loci, also highlights a  
284 level of sensitivity as well as an area for further investigation in our transcriptome. We have more than  
285 two times more complex loci, using NCBI as a reference, than Hestand. The inflated ISME complex loci  
286 numbers could be attributed to the double reporting of their transcripts. Awareness of these complex  
287 loci allows for refinement of transcriptome-wide gene structure, while a pipeline to appropriately  
288 process these loci has yet to be established. The evaluation of these alternative descriptive statistics  
289 permits comparisons with transcriptomes that have pipeline-specific limitations.

290 Accurate identification of UTRs is often difficult for *ab initio* programs and requires sufficient  
291 support of transcription evidence. Our integrative analysis of several tissues using different library preps  
292 enabled us to achieve unprecedented extension of equine transcripts' UTRs by an average of 3.3 kb per  
293 transcript. Indeed high coverage of CNS tissues in our analysis was an important factor as reported  
294 previously with several transcriptomes [20], [21] and [22]. Further improvements to this transcriptome  
295 would include providing tissue-specific UTR lengths and allowing for a more clear depiction of  
296 differences in gene structure between tissues. The improved UTR structure provided by our  
297 transcriptome has already shown its utility in the horse community by defining isoform and gene  
298 boundaries of *MUTYH* and *TOEI* [23] as well as providing an alternative start exon for *CYP7A1* [13]

299 The distinct RNA-seq libraries from eight tissues, allow us to extract tissue-specific features  
300 regarding gene expression, isoform usage and mitochondrial gene expression. Tissue specificity, in  
301 terms of gene expression, was demonstrated on two levels, first as biases in exon usage, especially one

302 and two exon gene expression in the embryo (Supplementary Table 3). Second, gene clustering and  
303 Panther annotation revealed inherent functions associated with each tissue (Figure 3A, Supplementary  
304 Table 5). The retina displayed the most uniquely present and absent isoforms, in agreement with other  
305 studies [25], and had correlated isoform annotations unique to the retina: visual perception and  
306 photoreceptor cell differentiation. The skeletal muscle was a tissue with a relatively low amount of  
307 unique tissue-specific isoforms, however, it shows utility of these isoforms with relatively high  
308 cumulative expression values (Figure 3B) as well as comparable splicing rates (Table 3). Three tissues:  
309 retina, skin, and embryo, had shorter read lengths and were not prepared as stranded libraries and thus  
310 these data may be artificially understated in terms of transcriptome complexity. In addition to the  
311 nuclear gene expression, the amount of transcription occurring from the mitochondrial chromosome can  
312 show how much of the sequencing resources are being allocated to genes of mitochondrial origin.  
313 Across the eight tissues, one would expect the tissue with the largest numbers of mitochondria to have  
314 the largest proportion of mitochondrial allocated transcriptional output [2]. Our data demonstrates these  
315 trends in the brainstem, skeletal muscle and spinal cord, however the cerebellum and retina do show an  
316 unexpectedly low mitochondrial gene load (Figure 3C). Further research establishing the relationship  
317 between the amount of mitochondria processed in a sample for RNA-seq and the resulting mitochondrial  
318 expression loads would be beneficial to understanding how much of the transcriptional output is  
319 dominated by an individual mitochondrion.

320 We identified 7494 candidate novel transcripts. These novel transcripts are selected based on  
321 having no overlap with genes in current equine annotation and authenticated by their protein-coding  
322 ability and/or overlap with aligned non-horse genes or *ab initio* gene predictions. Our novel transcripts  
323 have a diversity of coding exons in Category I and a particular expression bias in the embryonic tissues  
324 of Category II, in which a majority of these novel transcripts contain two exons (Figure 4C). The

325 Category I novel transcripts highlight the deficient equine ENSEMBL annotation, the need to pool the  
326 databases to get the most transcriptome coverage and the ability of our transcriptome to capture the  
327 potentially rare novel gene models (Figure 4A). Despite the ORF requirement for Category III novel  
328 transcripts, there is an obvious enrichment for single exon transcripts and a marked reduction of total  
329 transcription level (Figure 4C), which is indicative of non-coding RNA. Our novel gene analysis also  
330 produced a category of novel transcripts that were removed due to not having ORFs and were presumed  
331 to represent noisy transcription relating to primary transcripts, repetitive elements, sequencing errors and  
332 genome-based errors. The collection of Category III and these excluded novel transcripts may represent  
333 a repository of non-annotated non-coding RNA, which is an area that needs further annotation in the  
334 horse genome.

335 This transcriptome assembly pipeline not only produces flexible incorporation of additional  
336 transcriptomes, it also provides several products regarding levels of transcript filtering and  
337 appropriateness for downstream analysis. The different extractable transcriptome versions include  
338 transcriptomes after each individual filter, with the final refined transcriptome containing only genes  
339 with complete ORFs and genes aligning with other non-horse genes or *ab initio* gene predictions. A  
340 version of our transcriptome merged with NCBI and ENSEMBL annotations achieves breadth not  
341 covered by our tissues. These transcriptomes as well as the pipeline to make each of these  
342 transcriptomes are publically available on our GitHub repository. By making the workflow public and  
343 easy to execute and manipulate, we aim to expand the spectrum of tissues embodying this transcriptome  
344 and eliminate biases in annotated genes and thus downstream differential gene analysis. Increasing and  
345 providing the option for tissue-specific transcriptomes, allows for more targeted and refined usage of a  
346 certain tissue's transcriptome for differential gene analysis, resulting in downstream analysis of more  
347 significant differentially expressed genes. As stated in our overall goals of this project, we have

348 provided a framework for further improving the equine transcriptome and produced an equine  
349 transcriptome that expands on current equine annotations in the manner of UTR extension, isoform  
350 detection and novel gene identification.

351

## 352 **Methods**

353

### 354 *RNA-seq library preparation*

355

356 A total of twelve RNA-seq libraries in 8 tissues from 59 individuals (20 female, 27 males and 12  
357 embryos) were used to prepare our transcriptome. The brainstem, spinal cord and cerebellum were  
358 strand-specific 100 bp paired-end (PE) libraries. The skeletal muscle tissues were strand-specific PE125  
359 bp libraries. A subset of the embryo ICM (3 samples) and TE (3 samples) were unstranded PE100 bp  
360 libraries, the other subset (3 ICM and 3 TE) consisted of single end (SE) 100 bp reads. The retina RNA-  
361 seq libraries were unstranded SE80 bp libraries. And the skin libraries were all unstranded and consisted  
362 of PE80 bp, SE80bp and SE95 bp reads. The brainstem, spinal cord and cerebellum RNA libraries were  
363 all rRNA-depleted, the skin, retina and skeletal muscle libraries were poly-A captured. The embryonic  
364 libraries were neither poly-A selected nor rRNA depleted, they were prepared with the Ovation® RNA-  
365 seq System V2 (NuGEN, San Carlos, CA, USA), which aims to amplify mRNA as well as non-  
366 polyadenylated transcripts. Table 1 summarizes the tissue-specific RNA-seq library parameters.

367

368

### 369 *Trimming and Mapping of Reads*

370

371 The Illumina adaptors as well as the reads were trimmed with the sliding window quality  
372 trimmer Trimmomatic [26] with a window size of 4 and a softer quality threshold of 2 [27]. Mapping of  
373 the trimmed reads was done with Tophat2 [28] to EquCab2.0, 2007  
374 (<ftp://hgdownload.cse.ucsc.edu/goldenPath/equCab2>). Cufflinks [15] was used to assemble transcripts  
375 from the aligned RNA-Seq reads. Two cerebellar samples failed assembly due to computation  
376 limitations (8 CPUs, 250 Gb RAM and 7 days) and required digital normalization [29] to 200X coverage  
377 before mapping with Tophat2.

378

379

### 380 *Filtering Transcripts*

381

382 Four categories of filters were used to remove likely pre-mRNA and artifactual transfrags, as  
383 summarized in Figure 1, resulting in six versions of the transcriptome. Primary transcript filtration was  
384 done using Cuffcompare [15] between our assembly and a version of our assembly containing only  
385 multi-exon transcripts and removing transcripts overlapping with intronic regions and with class codes  
386 “i”, “e” and “o”. The input trimmed RNA-seq reads were then back-mapped to the pre-mRNA free  
387 transcriptome using the quasi-mapping based software package Salmon [30]. While back-mapping, a  
388 second filtration step was implemented: low abundance transcripts in every locus were excluded with  
389 the lower threshold of a TPM (normalized read count standing for transcripts per million) less than 5%  
390 of the total TPM per locus. For the third filter, Transdecoder [31] was used to predict the ORFs and  
391 Cuffcompare [15] to determine any exonic overlap with any candidate gene locus using the class codes  
392 “j”, “o”, “x” and “c”. In the Transdecoder analysis, the longest open reading frames were extracted as  
393 well as any sequences having significant homology to the Pfam and Swissprot protein databases.



394 Finally, the removal of likely erroneous mitochondrial and short transcripts was done by a homemade  
395 script.

396

### 397 *Transcriptome Comparisons*

398

399 Comparisons of our refined transcriptome to the four public horse transcriptomes were done  
400 using Cuffcompare [15]. In any pairwise comparison, two transcripts are considered matching if they  
401 have the exact intron chain, despite differing terminal exons (class code “=”). If the transcripts are not  
402 matching but sharing one or more splice junctions (class code “j”), these would be considered similar  
403 transcripts. A transcript is considered novel if it does not overlap with any gene model in the 2<sup>nd</sup>  
404 reference assembly (class code “u”). All other class codes including any kind of overlap with a reference  
405 annotation on the opposite strand were considered as “other”. For more detailed descriptions of the class  
406 codes provided by Cuffcompare, please see their manual [15]. Complex loci were flagged if a gene  
407 model of one assembly overlapped with 2 different gene models in the other assembly. Sensitivity and  
408 specificity relative to a given reference transcriptome were calculated per base, intron and locus for each  
409 transcriptome and reference combination as described by Burset and Guigó [14].

410

### 411 *Novel Gene Prediction*

412

413 Any transcript in our final *refined* transcriptome is defined as novel if it does not overlap with a  
414 gene model in at least one of the two public equine assemblies, NCBI and ENSEMBL (Cuffcompare  
415 class code “u”). Transcripts considered novel were divided into three groups according to the degree of  
416 supportive evidence. Transcripts novel to either the NCBI or ENSEMBL assemblies with transcriptional

417 supportive evidence from the other or any other public assembly [5, 7] were in the first category of  
418 novel transcripts. Supportive evidence is defined as any overlapping with exon sequence (Cuffcompare  
419 class code “=”, “j”, “o”, “x” or “c”). The second and third categories of novel transcripts required that the  
420 transcript be absent in all current equine transcriptomes. Transcripts in the second category have  
421 supportive evidences in non-horse alignment gene models or *ab initio* gene prediction tracks from the  
422 UCSC genome browser. The third category of novel transcripts included transcripts that lack such  
423 evidence but have ORFs.

424

#### 425 *Tissue-Specific Characterization of The Transcriptome*

426

427 Tissue-specific transcriptomes were generated by back-mapping the input trimmed RNA-seq  
428 reads with Salmon [30] to the refined version of the transcriptome to obtain expression information on a  
429 tissue-specific level. A transcript is considered expressed in a given tissue if it has a TPM more than 5%  
430 of the total TPM per locus calculated from the tissue specific libraries only. Biological processes  
431 identified within the tissue-specific gene blocks were annotated with Panther [32] and reported if the p-  
432 values were below the Bonferroni-corrected threshold (5% experiment-wide).

433

#### 434 *UCSC Track hubs*

435

436 Gene Annotation Format (GTF) files were converted into the binary bigbed files [33] using  
437 UCSC kintUtils (<https://github.com/ENCODE-DCC/kentUtils>). The track hub directory structure was  
438 designed as recommend by UCSC genome browser [34]. Tracks were constructed using “bigBed 12”  
439 format and multiple libraries of the same tissue were organized in composite tracks. The hub files are

440 hosted on a github server as a part of the horse\_trans repository ([https://github.com/dib-lab/horse\\_trans](https://github.com/dib-lab/horse_trans)).

441

442 **List of Abbreviations:**

443 Single Nucleotide polymorphism (SNP)

444 Untranslated region (UTR)

445 Central nervous system (CNS)

446 Inner cell mass (ICM)

447 Trophectoderm (TE)

448 RNA sequencing (RNA-seq)

449

450

451 **Declarations**

452 *Ethics approval and consent to participate*

453 Not applicable

454 *Consent for publication*

455 All consent for publication is available

456 *Availability of data and materials*

457 The data including the scripts for the pipeline as well as the GTF files for the transcriptome can be found

458 at: [https://github.com/dib-lab/horse\\_trans](https://github.com/dib-lab/horse_trans). (This repository is archived by Zenodo at

459 10.5281/zenodo.56934). All sequencing reads used in this study have been submitted to NCBI

460 Sequence Read Archive; SRA SRP082284 for muscle samples, SRP073514 for brainstem, SRP073514

461 and SRP082291 for spinal cord, SRP082342 for cerebellum, ERP001525 for retina, SRP031504 and

462 SRP082454 for embryonic tissues and ERP001524, ERP001525 and ERP005568 for skin.

463  
464 *Competing Interests*

465       The authors declare that there are no competing interests.

466 *Funding*

467       Support for the spinal cord and brainstem work was provided by the National Institutes of Health  
468 (NIH) to C.J.F. (1K01OD015134-01A1 and L40 TR001136). Additional postdoctoral fellowship support  
469 was provided by the Morris Animal Foundation (D14EQ-021) to C.J.F..

470 *Authors' Contributions*

471       All authors contributed to study conception and design. TAM produced the annotation pipeline  
472 and did the data analysis with oversight on writing of the manuscript as well as figure formation. EYS  
473 wrote the manuscript and made the figures. CTB, CJF and JDM aided with experimental design and  
474 supervised the whole project. RRB and MJM provided retina and skin data. SJV provided muscle data.  
475 PJR provided both embryonic tissue data. CJF provided spinal cord and brainstem data. EYS, JDM and  
476 MCP provided the cerebellar RNA-seq data. All authors reviewed and approved the final version of the  
477 manuscript.

478 *Acknowledgements*

479       We would like to thank the Arabian horse foundation and Henry Jastro Shields awards for work  
480 done on the cerebellum. For the embryo work, support was given by Centre for Equine Health, UC  
481 Davis. University of Minnesota Equine Center supported the muscle transcriptomic work used for this  
482 study. The RNA seq data from skin and retina was supported in part by generous donations by  
483 Appaloosa breeders who belong to the Appaloosa Project's Electronic Classroom and by the L. David

484 Dube and Heather Ryan Veterinary Health Research Fund from the University of Saskatchewan. For  
485 J.D.M., M.J.M. and P.J.R. support was provided by UC Davis Agriculture Experiment Station.

486  
487

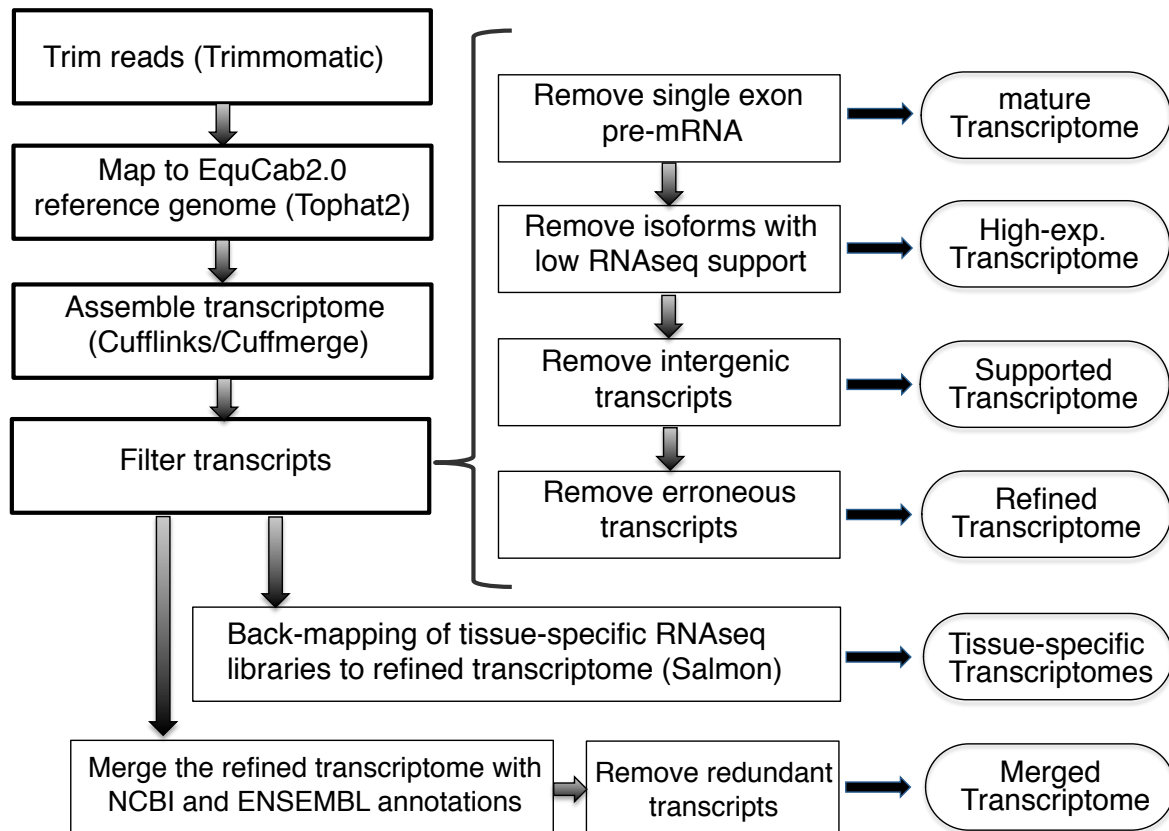
## References

488

- 489 1. Brown JB, Boley N, Eisman R, May GE, Stoiber MH, Duff MO, Booth BW, Wen J, Park S,  
490 Suzuki AM *et al*: **Diversity and dynamics of the *Drosophila* transcriptome.** *Nature* 2014,  
491 **512**(7515):393-399.
- 492 2. Mele M, Ferreira PG, Reverter F, DeLuca DS, Monlong J, Sammeth M, Young TR, Goldmann  
493 JM, Pervouchine DD, Sullivan TJ *et al*: **Human genomics. The human transcriptome**  
494 **across tissues and individuals.** *Science* 2015, **348**(6235):660-665.
- 495 3. Okazaki Y, Furuno M, Kasukawa T, Adachi J, Bono H, Kondo S, Nikaido I, Osato N, Saito R,  
496 Suzuki H *et al*: **Analysis of the mouse transcriptome based on functional annotation of**  
497 **60,770 full-length cDNAs.** *Nature* 2002, **420**(6915):563-573.
- 498 4. Holl HM, Gao S, Fei Z, Andrews C, Brooks SA: **Generation of a de novo transcriptome**  
499 **from equine lamellar tissue.** *BMC Genomics* 2015, **16**(1):739.
- 500 5. Pacholewska A, Drogemuller M, Klukowska-Rotzler J, Lanz S, Hamza E, Dermitzakis ET,  
501 Marti E, Gerber V, Leeb T, Jagannathan V: **The transcriptome of equine peripheral blood**  
502 **mononuclear cells.** *PLoS One* 2015, **10**(3):e0122011.
- 503 6. Coleman SJ, Zeng Z, Wang K, Luo S, Khrebtukova I, Mienaltowski MJ, Schroth GP, Liu J,  
504 MacLeod JN: **Structural annotation of equine protein-coding genes determined by**  
505 **mRNA sequencing.** *Anim Genet* 2010, **41 Suppl 2**:121-130.
- 506 7. Hestand MS, Kalbfleisch TS, Coleman SJ, Zeng Z, Liu J, Orlando L, MacLeod JN: **Annotation**  
507 **of the Protein Coding Regions of the Equine Genome.** *PLoS One* 2015, **10**(6):e0124375.
- 508 8. Yandell M, Ence D: **A beginner's guide to eukaryotic genome annotation.** *Nat Rev Genet*  
509 2012, **13**(5):329-342.
- 510 9. Curwen V, Eyraas E, Andrews TD, Clarke L, Mongin E, Searle SM, Clamp M: **The Ensembl**  
511 **automatic gene annotation system.** *Genome Res* 2004, **14**(5):942-950.
- 512 10. Kitts P: **The NCBI Handbook: Chapter 14. Genome Assembly and Annotation Process.**  
513 In: *National Center for Biotechnology.* 2003 edn: McEntyre, J. & Ostell, J.; 2003.
- 514 11. Taanman JW: **The mitochondrial genome: structure, transcription, translation and**  
515 **replication.** *Biochim Biophys Acta* 1999, **1410**(2):103-123.
- 516 12. Plotz G, Casper M, Raedle J, Hinrichsen I, Heckel V, Brieger A, Trojan J, Zeuzem S: **MUTYH**  
517 **gene expression and alternative splicing in controls and polyposis patients.** *Hum*  
518 *Mutat* 2012, **33**(7):1067-1074.
- 519 13. Finno CJ, Bordbari M, Monsour T, Bannasch DL, Mickelson DB, Valberg SJ: **Spinal cord**  
520 **transcriptome profiling of equine vitamin E deficient neuroaxonal dystrophy**  
521 **identifies dysregulation of cholesterol homeostasis with upregulation of liver X**  
522 **receptor target genes.** *In Review, Free Rad Biol Med* 2016.
- 523 14. Burset M, Guigo R: **Evaluation of gene structure prediction programs.** *Genomics* 1996,  
524 **34**(3):353-367.

- 525 15. Trapnell C, Hendrickson DG, Sauvageau M, Goff L, Rinn JL, Pachter L: **Differential analysis**  
526 **of gene regulation at transcript resolution with RNA-seq.** *Nat Biotechnol* 2013,  
527 **31(1):46-53.**
- 528 16. Bertone P, Stolc V, Royce TE, Rozowsky JS, Urban AE, Zhu X, Rinn JL, Tongprasit W, Samanta  
529 M, Weissman S *et al*: **Global identification of human transcribed sequences with**  
530 **genome tiling arrays.** *Science* 2004, **306(5705):2242-2246.**
- 531 17. Khaitovich P, Kelso J, Franz H, Visagie J, Giger T, Joerchel S, Petzold E, Green RE, Lachmann  
532 M, Paabo S: **Functionality of intergenic transcription: an evolutionary comparison.**  
533 *PLoS Genet* 2006, **2(10):e171.**
- 534 18. Schadt EE, Edwards SW, GuhaThakurta D, Holder D, Ying L, Svetnik V, Leonardson A, Hart  
535 KW, Russell A, Li G *et al*: **A comprehensive transcript index of the human genome**  
536 **generated using microarrays and computational approaches.** *Genome Biol* 2004,  
537 **5(10):R73.**
- 538 19. Sultan M, Amstislavskiy V, Risch T, Schuette M, Dokel S, Ralser M, Balzereit D, Lehrach H,  
539 Yaspo ML: **Influence of RNA extraction methods and library selection schemes on**  
540 **RNA-seq data.** *BMC Genomics* 2014, **15:675.**
- 541 20. Smibert P, Miura P, Westholm JO, Shenker S, May G, Duff MO, Zhang D, Eads BD, Carlson J,  
542 Brown JB *et al*: **Global patterns of tissue-specific alternative polyadenylation in**  
543 **Drosophila.** *Cell Rep* 2012, **1(3):277-289.**
- 544 21. Mangone M, Manoharan AP, Thierry-Mieg D, Thierry-Mieg J, Han T, Mackowiak SD, Mis E,  
545 Zegar C, Gutwein MR, Khivansara V *et al*: **The landscape of C. elegans 3'UTRs.** *Science*  
546 2010, **329(5990):432-435.**
- 547 22. Ulitsky I, Shkumatava A, Jan CH, Subtelny AO, Koppstein D, Bell GW, Sive H, Bartel DP:  
548 **Extensive alternative polyadenylation during zebrafish development.** *Genome Res*  
549 2012, **22(10):2054-2066.**
- 550 23. Scott EY, Penedo MC, Murray JD, Finno CJ: **Defining Trends in Global Gene Expression in**  
551 **Arabian Horses with Cerebellar Abiotrophy.** *In Review, Cerebellum* 2016.
- 552 24. Wu JQ, Habegger L, Noisa P, Szekely A, Qiu C, Hutchison S, Raha D, Egholm M, Lin H,  
553 Weissman S *et al*: **Dynamic transcriptomes during neural differentiation of human**  
554 **embryonic stem cells revealed by short, long, and paired-end sequencing.** *Proc Natl*  
555 *Acad Sci U S A* 2010, **107(11):5254-5259.**
- 556 25. Farkas MH, Grant GR, White JA, Sousa ME, Consugar MB, Pierce EA: **Transcriptome**  
557 **analyses of the human retina identify unprecedented transcript diversity and 3.5 Mb**  
558 **of novel transcribed sequence via significant alternative splicing and novel genes.**  
559 *BMC Genomics* 2013, **14:486.**
- 560 26. Bolger AM, Lohse M, Usadel B: **Trimmomatic: a flexible trimmer for Illumina sequence**  
561 **data.** *Bioinformatics* 2014, **30(15):2114-2120.**
- 562 27. Macmanes MD: **On the optimal trimming of high-throughput mRNA sequence data.**  
563 *Front Genet* 2014, **5:13.**
- 564 28. Kim D, Pertea G, Trapnell C, Pimentel H, Kelley R, Salzberg SL: **TopHat2: accurate**  
565 **alignment of transcriptomes in the presence of insertions, deletions and gene**  
566 **fusions.** *Genome Biol* 2013, **14(4):R36.**
- 567 29. Brown C, Howe, A., Zhang, Q., Pyrkosz, A.B. & Brom, T.H.: **A Reference-Free Algorithm for**  
568 **Computational Normalization of Shotgun Sequencing Data.** 2013.
- 569 30. Rob Patro GD, Carl Kingsford: **Accurate, fast, and model-aware transcript expression**  
570 **quantification with Salmon.** *bioRxiv* 2015.

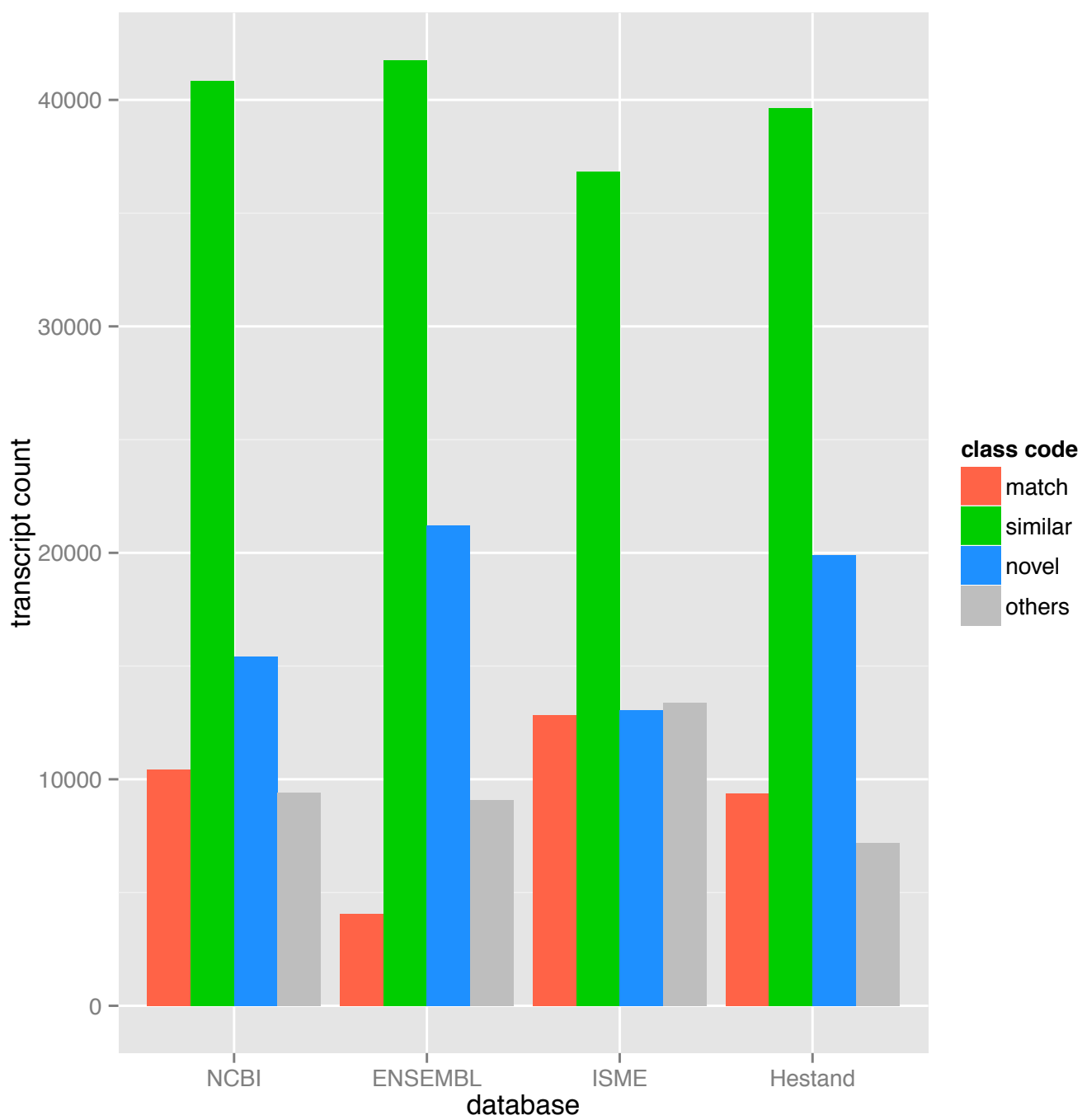
- 571 31. Haas BJ, Papanicolaou A, Yassour M, Grabherr M, Blood PD, Bowden J, Couger MB, Eccles D,  
572 Li B, Lieber M *et al*: **De novo transcript sequence reconstruction from RNA-seq using**  
573 **the Trinity platform for reference generation and analysis.** *Nat Protoc* 2013,  
574 **8(8):1494-1512.**
- 575 32. Mi H, Muruganujan A, Casagrande JT, Thomas PD: **Large-scale gene function analysis**  
576 **with the PANTHER classification system.** *Nat Protoc* 2013, **8(8):1551-1566.**
- 577 33. Kent WJ, Zweig AS, Barber G, Hinrichs AS, Karolchik D: **BigWig and BigBed: enabling**  
578 **browsing of large distributed datasets.** *Bioinformatics* 2010, **26(17):2204-2207.**
- 579 34. Raney BJ, Dreszer TR, Barber GP, Clawson H, Fujita PA, Wang T, Nguyen N, Paten B, Zweig  
580 AS, Karolchik D *et al*: **Track data hubs enable visualization of user-defined genome-**  
581 **wide annotations on the UCSC Genome Browser.** *Bioinformatics* 2014, **30(7):1003-1005.**  
582  
583  
584  
585  
586  
587  
588  
589  
590  
591  
592  
593  
594  
595  
596  
597  
598  
599  
600  
601  
602  
603  
604  
605  
606  
607  
608  
609  
610  
611  
612  
613  
614  
615  
616

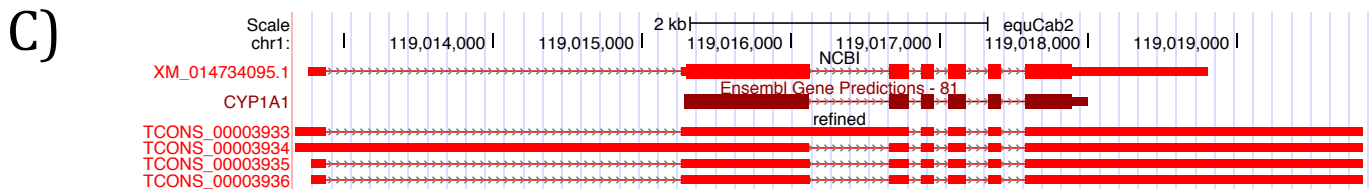
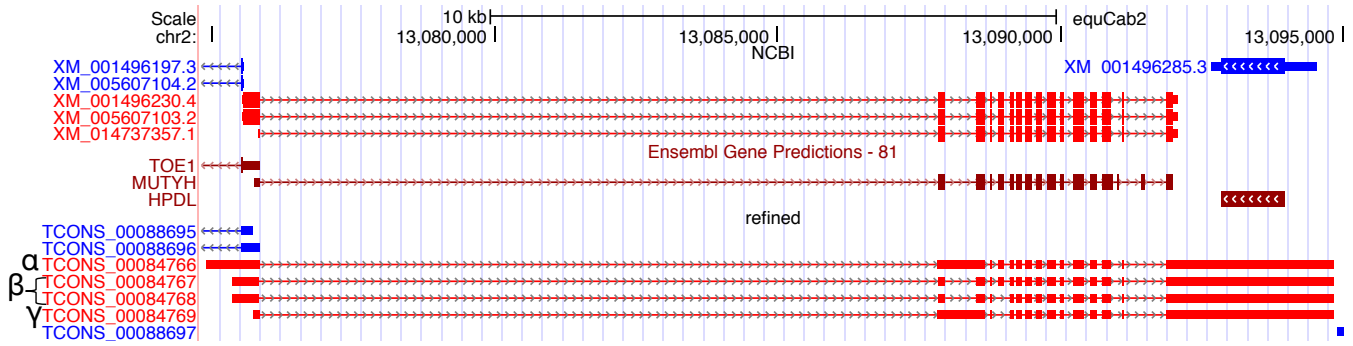


**Figure 1.** An outline of the workflow used to generate each version of the transcriptome. Transcriptome products are in ovals. Programs used to perform various steps are indicated in parentheses. All transcriptome versions and the pipeline scripts are publically available.



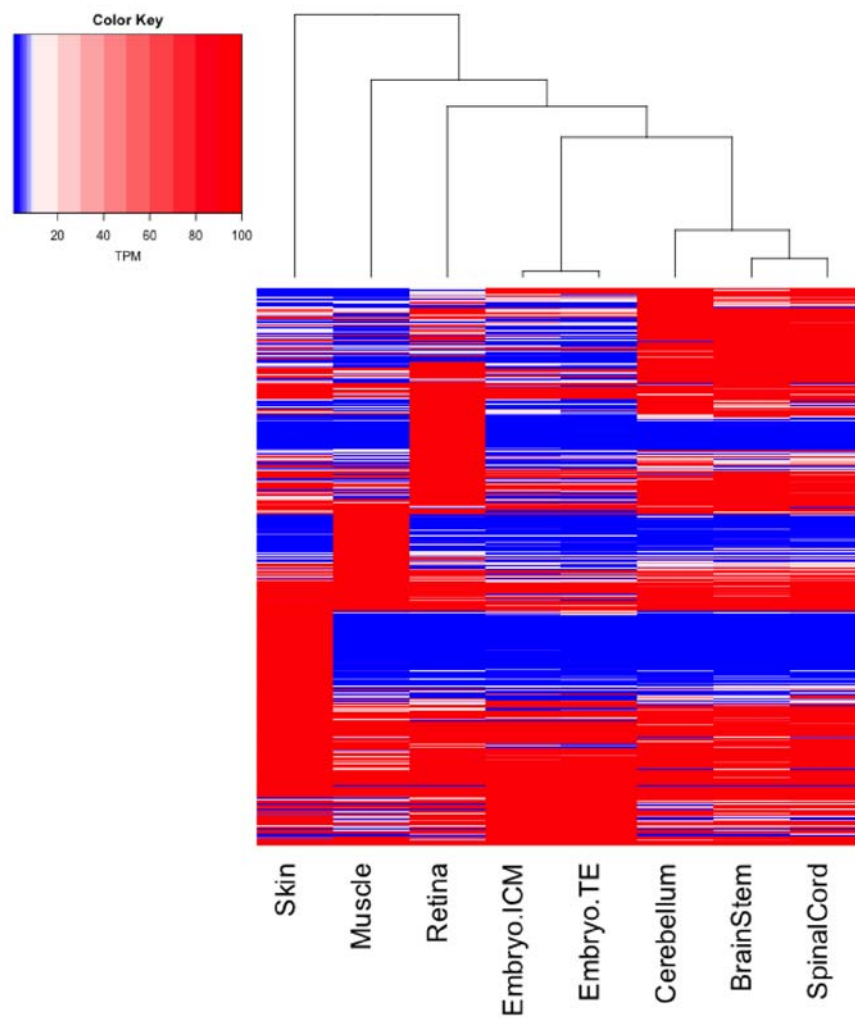
A)

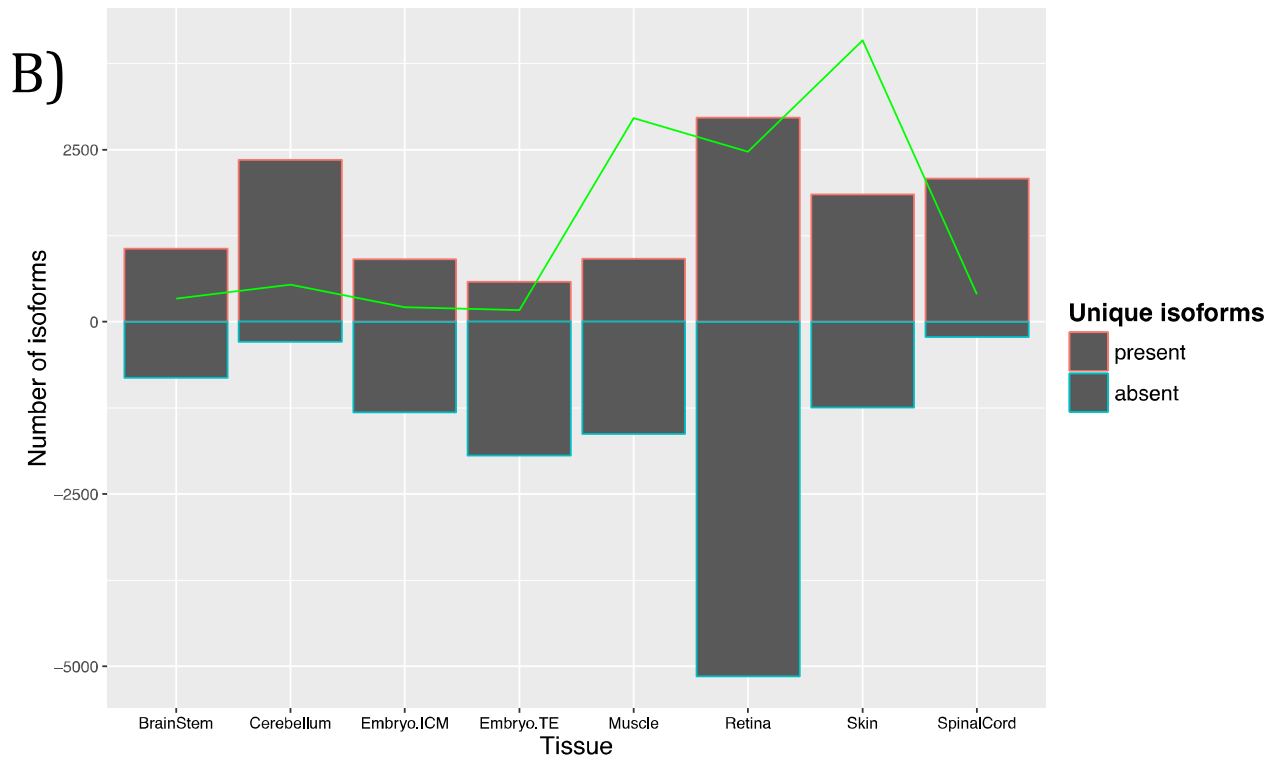




**Figure 2.** Comparison of our refined transcriptome to current equine annotations. (A) Our refined transcriptome compared to current annotations. (B) The annotation of *MUTYH* in the refined version of the transcriptome shows the addition of several isoforms,  $\alpha$ ,  $\beta$ , and  $\gamma$ , as seen in the human, of *MUTYH*. (C) The gene annotation of *CYP7A1* in the refined transcriptome also shows the inclusion of an extended alternative first exon not seen in other species.

A)





C)

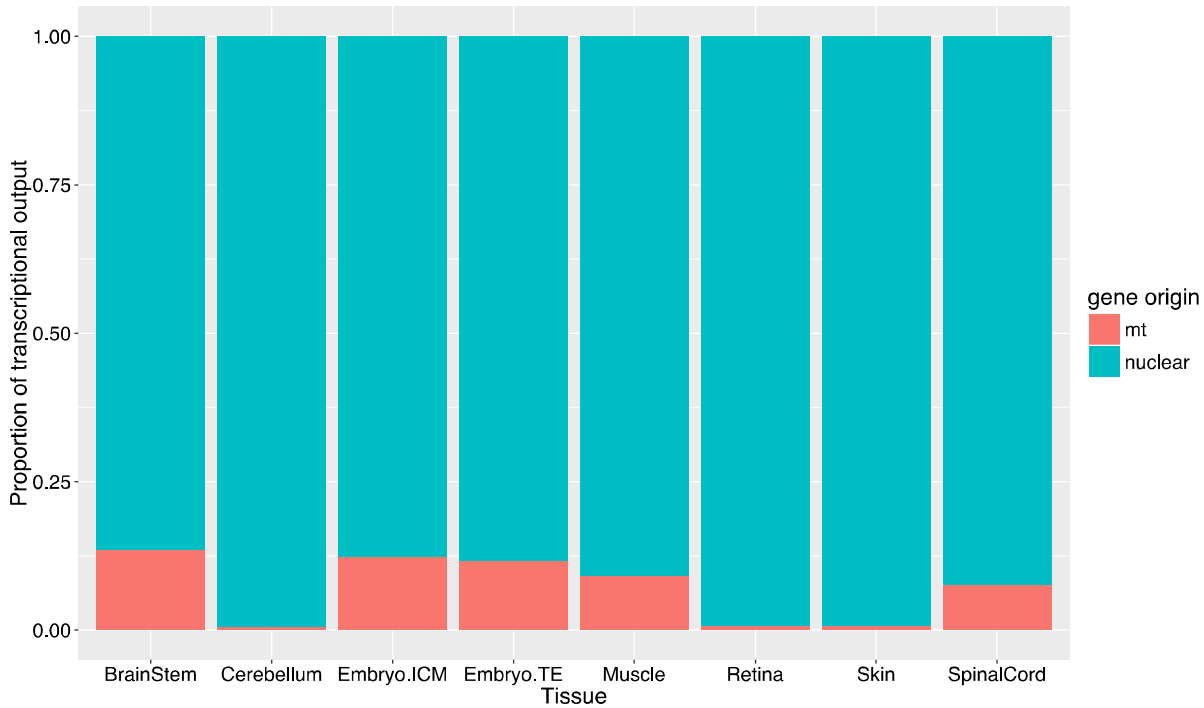
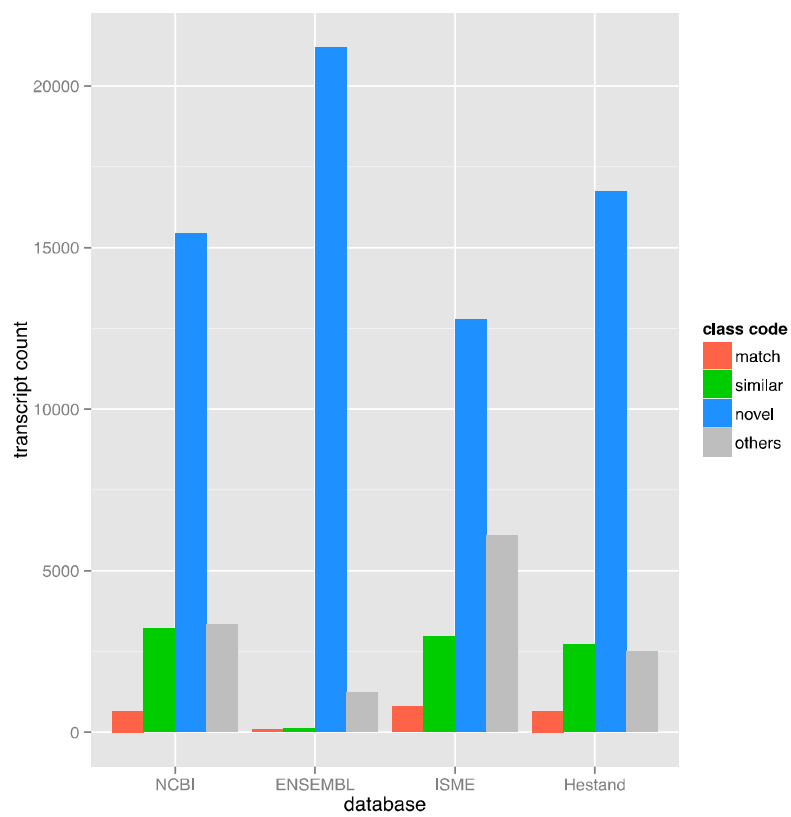
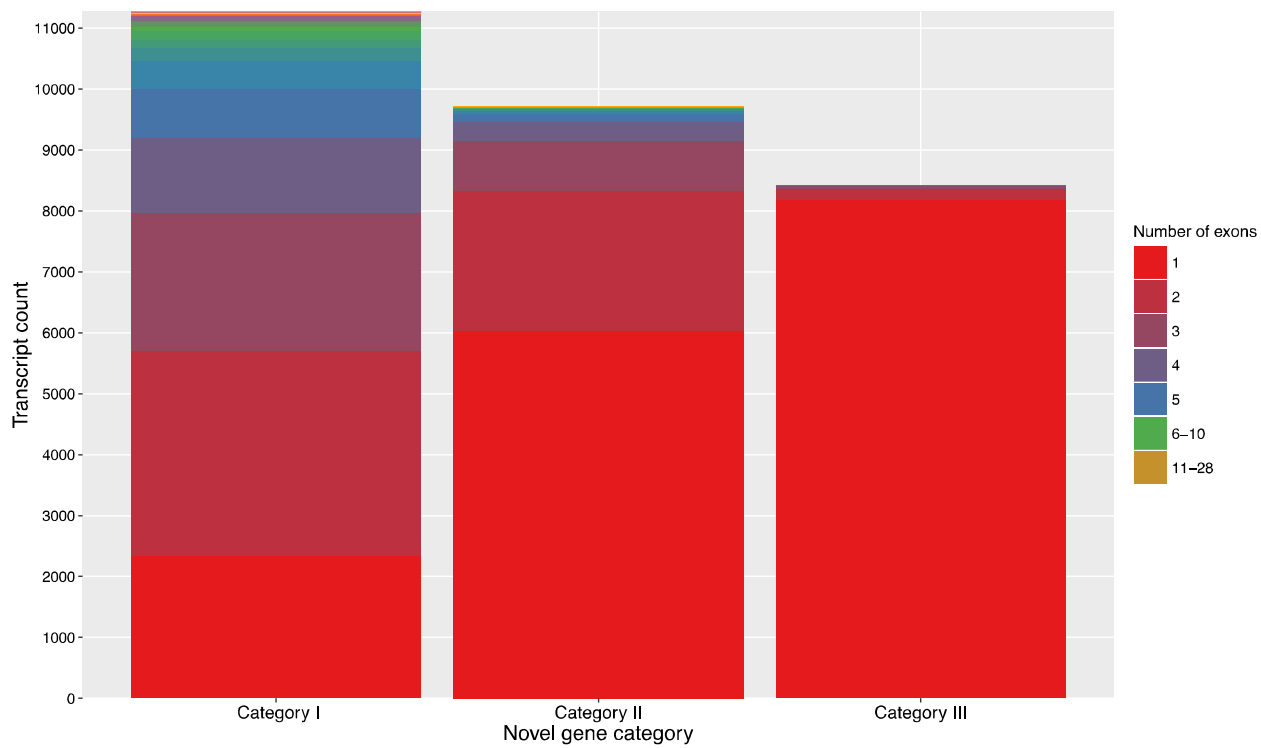


**Figure 3.** Tissue-specific gene and isoform composition of the transcriptome. (A) A heatmap of genes with high expression and substantial expression differences across tissues. (B) A bar graph showing isoforms uniquely present (the bar outlined in red above the x-axis) or solely absent (the blue outlined bars extending below the x-axis). The green trendline corresponds to the cumulative TPM of the uniquely present transcripts. (C) A stacked bar graph showing the transcription percentage of mitochondrial genes versus nuclear encoded genes.

A)



B)



C)

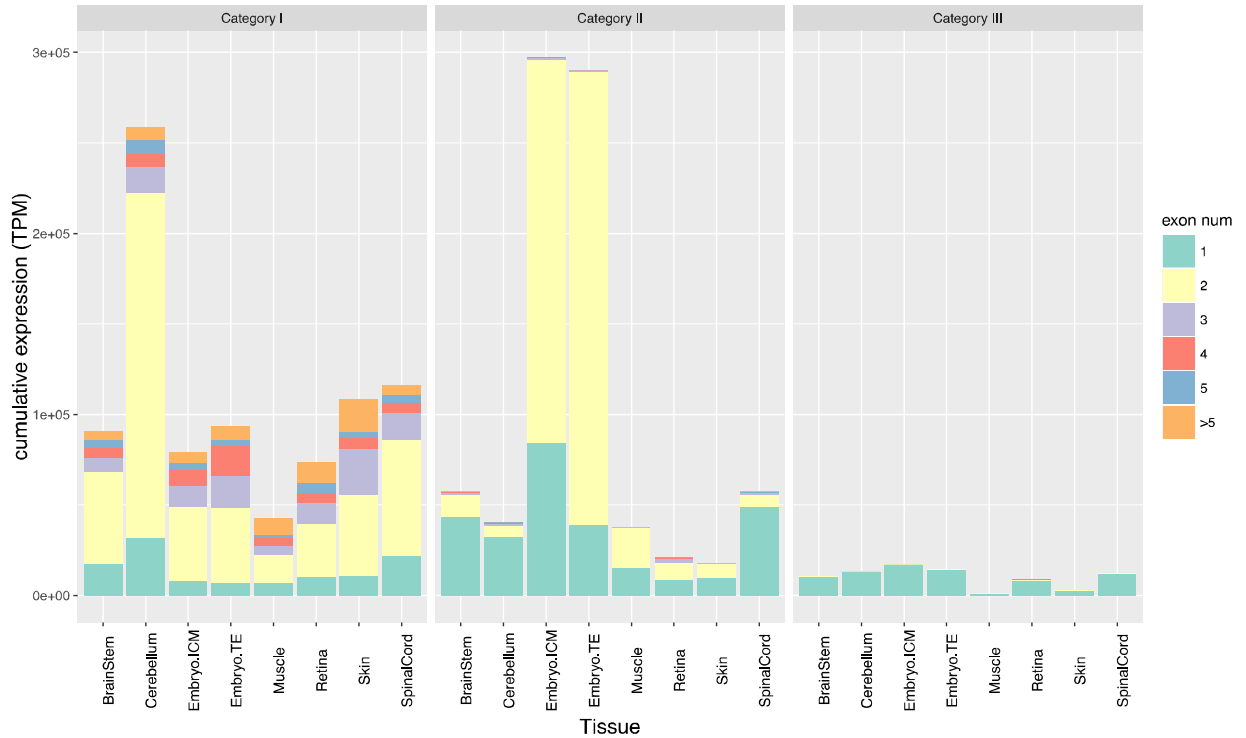


**Figure 4.** Novel gene analysis and classification. (A) A bar graph showing the comparison of all the novel genes against the current equine annotations. The three categories of novel genes were supported novel genes (Category I), unsupported, but conserved, novel genes (Category II) and the unsupported, un-conserved, but novel genes with an ORF (Category III). (B) A stacked bar graph of transcript counts with all three categories of novel genes showing exonic composition and (C) their cumulative TPM in a tissue specific manner.



**Table 1.** Sample and library preparations used as input for our equine transcriptome.

| Tissue     | Library Preparation | Library Characteristics | #Samples | #Frag(M) | #bp(Gb) | Reference           |
|------------|---------------------|-------------------------|----------|----------|---------|---------------------|
| BrainStem  | RiboRNA-depleted    | PE100bp, stranded       | 8*       | 166.73   | 33.68   | Finno et al, 2016   |
| Cerebellum | RiboRNA-depleted    | PE100bp, stranded       | 12       | 411.48   | 82.3    | Scott et al, 2016   |
| Muscle     | Poly-A capture      | PE125bp, stranded       | 12       | 301.94   | 76.08   |                     |
| Retina     | Poly-A captured     | PE80bp unstranded       | 2        | 20.3     | 3.28    | Bellone et al, 2013 |
| SpinalCord | RiboRNA-depleted    | PE100bp, stranded       | 16*      | 403      | 81.4    | Finno et al, 2016   |
| Skin       | Poly-A captured     | PE80bp, unstranded      | 2        | 18.54    | 3       | Holl et al, 2016    |
|            | Poly-A captured     | SE80bp, unstranded      | 2        | 16.57    | 1.34    | Holl et al, 2016    |
|            | Poly-A captured     | SE95bp unstranded       | 3        | 105.51   | 10.02   | Bellone et al, 2013 |
| Embryo ICM | Ovation RNA-seq     | PE100bp, unstranded     | 3        | 126.32   | 25.26   | Iqbal et al, 2014   |
|            | Ovation RNA-seq     | SE100bp, unstranded     | 3        | 115.21   | 11.52   | Iqbal et al, 2014   |
| Embryo TE  | Ovation RNA-seq     | PE100bp, unstranded     | 3        | 129.84   | 25.96   | Iqbal et al, 2014   |
|            | Ovation RNA-seq     | SE100bp, unstranded     | 3        | 102.26   | 10.23   | Iqbal et al, 2014   |
| Total      |                     |                         | 69       | 1917.7   | 364.07  |                     |

\*Seven individuals had both brainstem and spinal cord tissue collected from them. Seven of the skin samples were taken from 5 individuals and one individual had both retina and skin sampled, bringing our total number of individuals to 59.

**Table 2.** Comparison of current public equine annotations to six versions of our transcriptome (bolded and outline in red) in terms of gene numbers and composition

|                         | <b>Unfiltered</b> | <b>Mature</b> | <b>High-exp</b> | <b>Supported</b> | <b>Refined</b> | <b>Merged</b> | Hestand | ISME   | NCBI  | ENSEMBL |
|-------------------------|-------------------|---------------|-----------------|------------------|----------------|---------------|---------|--------|-------|---------|
| Genes (super-loci)      | 117019            | 75102         | 75375           | 37062            | 36876          | 47760         | 56495   | 42654  | 24342 | 26962   |
| Transcripts             | 211562            | 162261        | 114830          | 76323            | 76125          | 121997        | 68594   | 285538 | 43417 | 29196   |
| Multi-transcript loci   | 17136             | 15430         | 14602           | 14511            | 14505          | 17835         | 8465    | 23833  | 7257  | 1592    |
| Multi-exon transcripts  | 108985            | 108985        | 61570           | 60839            | 60782          | 97654         | 30949   | 259556 | 39272 | 19805   |
| Redundant transcripts   | 0                 | 0             | 0               | 0                | 0              | 2             | 3       | 12578  | 141   | 79      |
| Unstranded transcripts  | 46928             | 35881         | 35872           | 6676             | 6618           | 5705          | 37673   | 4732   | 0     | 0       |
| Single exon transcripts | 102577            | 53276         | 53260           | 15484            | 15343          | 24341         | 37642   | 13404  | 3723  | 6862    |
| Two exons transcripts   | 11114             | 11114         | 9449            | 8857             | 8808           | 11350         | 4410    | 13092  | 2425  | 2972    |
| Many exons transcripts  | 97871             | 97871         | 52121           | 51982            | 51974          | 86306         | 26542   | 259042 | 37269 | 19362   |

**Table 3.** Tissue-specific splicing rate as calculated by Cuffcompare, with relevant number of multi-exonic transcripts and multi-transcript loci per tissue.

|                        | Embryo ICM | Embryo TE | Skin  | Brainstem | Cerebellum | Retina | Spinal cord | Muscle |
|------------------------|------------|-----------|-------|-----------|------------|--------|-------------|--------|
| Genes                  | 33998      | 32050     | 30003 | 34792     | 36139      | 26733  | 34980       | 29549  |
| transcripts            | 57400      | 54424     | 51995 | 62993     | 66364      | 47095  | 66001       | 52000  |
| multi-exon transcripts | 44069      | 42433     | 42432 | 49346     | 51640      | 39420  | 52175       | 42483  |
| multi-transcript loci  | 11938      | 11461     | 11797 | 13066     | 13334      | 10866  | 13352       | 11560  |
| Splicing rate          | 1.7        | 1.7       | 1.7   | 1.8       | 1.8        | 1.8    | 1.9         | 1.8    |